High-pressure structural study of dolomite and ankerite

Nancy L. Ross
Department of Geological Sciences, University College London, Gower Street, London WC1E 6BT, U.K.

Richard J. Reeder
Mineral Physics Institute and Department of Earth and Space Sciences, State University of New York,
Stony Brook, New York 11794, U.S.A.

Abstract

Structural parameters have been refined using X-ray intensity data for a stoichiometric dolomite single crystal at room pressure and at 1.50, 2.90, 3.70, and 4.69 GPa; and for a single crystal of a ferroan dolomite with approximately 70 mol% $CaFe(CO_3)_2$ at room pressure and at 1.90, 2.97, and 4.0 GPa. The principal structural change with increasing pressure is compression of the CaO_6 and $(Mg,Fe)O_6$ octahedra. The CO_3 group remains essentially invariant throughout the pressure range studied. The effect of the polyhedral compression is reflected in the anisotropic compression of the unit-cell parameters. In both dolomite and ankerite, c is approximately three times as compressible as a.

In addition to displaying similar axial compressibilities, dolomite and ankerite display similar bond compressibilities and bulk moduli. The isothermal bulk modulus of dolomite determined from cell volume compression data, assuming the pressure derivative is 4, is 94 GPa, and that of ankerite is 91 GPa. The polyhedral bulk moduli of CaO_6 and $(Mg,Fe)O_6$ are also similar, with CaO_6 being slightly more compressible than $(Mg,Fe)O_6$. The latter has a greater compressibility than generally observed in other oxides and silicates. The distortion of the octahedra, though already small, decreases slightly with pressure. No phase change was observed in either compound throughout the pressure range studied.

Introduction

Relatively little is known about the structural behavior of carbonate minerals at conditions of high pressure and temperature. Most petrologic interest in calcium magnesium iron carbonates has been in the properties of the phases at near-surface conditions. However, metamorphic and igneous carbonates have also generated considerable interest, and in some cases the carbonates have provided important constraints on petrogenesis. There has been considerable debate concerning the possible role of carbonates in the upper mantle (e.g., Irving and Wyllie, 1973). Experimental phase equilibria studies demonstrate that dolomite is stable over a wide range of pressures and temperatures. Irving and Wyllie (1975) show the stability field of dolomite solid solution extending to approximately 1300 °C at 3.0 GPa, near the upper limit of pressure in their piston-cylinder experiments. The occurrence of dolomite and ferroan dolomite as major constituents in many carbonatites and the speculated existence of these phases in mantle carbonated peridotite raise questions concerning the crystal chemical behavior of carbonate minerals at lower crust and upper mantle conditions.

High-temperature crystal structures have been refined for three rhombohedral carbonates: calcite (up to 800 °C), magnesite (up to 500 °C), and dolomite (up to 600 °C) (Markgraf and Reeder, 1985; Reeder and Markgraf, 1986).

Rotational disordering of the CO_3 group in calcite has also been studied at high temperatures (Dove and Powell, 1989; Redfern et al., 1989). Of these carbonates, only calcite has been studied in any detail at high pressures. Calcite undergoes a displacive phase transition at room temperature and approximately 1.5 GPa to a monoclinic phase, $CaCO_3$-II, which itself transforms to another polymorph, $CaCO_3$-III, at approximately 2.2 GPa (Merrill and Bassett, 1975). Both high-pressure polymorphs are apparently metastable and exist within the stability field of aragonite.

In this study we report the results of structure refinements for dolomite and ankerite using X-ray intensity data obtained at high pressure in a diamond-anvil cell. Unlike calcite, no evidence for any phase transition was observed to 4.69 GPa in dolomite or to 4.00 GPa in ankerite. Possible factors leading to these contrasting structural responses to pressure are discussed, along with a comparison between the high-pressure and high-temperature behavior of dolomite.

Experimental method

Specimen description

The dolomite crystal used in this study was taken from a clear cleavage rhomb of Eugui dolomite. Eugui dolomite was selected for this study because of its high-quality single crystals and because it was used in earlier studies,

including the single-crystal deformation work of Barber et al. (1981), the refinements of thermally disordered dolomite by Reeder and Wenk (1983), and Reeder and Markgraf's (1986) high-temperature study. Eugui dolomite is fully ordered and the composition is nearly ideal, $Ca_{1.001}Mg_{0.987}Fe_{0.010}Mn_{0.002}(CO_3)_2$ (Reeder and Wenk, 1983). In addition, examination in the transmission electron microscope has shown that Eugui dolomite is homogeneous with relatively low dislocation densities (Barber et al., 1981; Reeder and Wenk, 1983). The crystal used in this study has approximate dimensions of $150 \times 62 \times 50$ μm. The crystal was selected after examination with the polarizing microscope, which showed that the crystal was clear, free of inclusions, and appeared to be a single crystal. Further examination on the diffractometer verified that the crystal is untwinned and has sharp, well-defined diffraction peak profiles.

The ankerite crystal used in this study, AMNH 8059, was taken from the same sample used by Reeder and Dollase (1989) in their study of the dolomite-ankerite solid solution series. The composition reported by those authors, on the basis of microprobe results, is $Ca_{0.997}Mg_{0.273}Fe_{0.676}Mn_{0.054}(CO_3)_2$. X-ray refinements of the site occupancies of the crystal chosen in this study agree with Reeder and Dollase's (1989) site refinements: the A site is filled with Ca and the B site is filled with 73% Fe (+ Mn) and 27% Mg. Several ankerite crystals were examined with the polarizing microscope and on the diffractometer. Each crystal examined either contained inclusions, was twinned, or both. We chose an inclusion-free crystal with approximate dimensions $75 \times 50 \times 50$ μm. Examination of the crystal on the diffractometer showed that the crystal is twinned with twin law $\{11\bar{2}0\}$. The parent to twin volume ratio determined from refinements (see below) is 1.0:0.27.

High-pressure data measurements

The procedure for studying single crystals at high pressure is described in detail by Hazen and Finger (1982). In brief, each crystal was mounted in a triangular Merrill-Bassett-type diamond-anvil cell with an INCONEL 750X gasket with a hole diameter of 350 μm. The crystal and a 15-μm chip of ruby pressure calibrant were affixed to one diamond face with a thin smear of the alcohol-insoluble fraction of vaseline, and a 4:1 mixture of non-dried methanol to ethanol was the hydrostatic pressure-transmitting medium. The pressure was calculated by measuring the shift of the R_1 fluorescence line of ruby relative to the room pressure reading before and after each experiment. The uncertainty is the pressure readings is ±0.05 GPa.

Unit-cell parameters of dolomite were obtained at 0.47, 1.50, 2.34, 2.90, 3.70, 4.20, and 4.69 GPa as well as at room pressure with the crystal mounted in the diamond-anvil cell. Similarly, unit-cell parameters of ankerite were measured at 0, 0.97, 1.90, 2.56, 2.97, 3.40, and 4.00 GPa. At each pressure, from 16 to 20 reflections with $20°$ $< 2\theta < 30°$ were centered at eight equivalent positions

TABLE 1. Data measurement and refinement information for dolomite at several pressures

Pressure (GPa)	No. ind. obs. ($>2\sigma_I$)	R	R_w	GOF
0.00	108	0.027	0.014	1.91
1.50	108	0.035	0.029	3.69
2.90	108	0.032	0.026	3.33
3.70	108	0.032	0.020	2.39
4.69	85	0.034	0.022	2.68

Note: $R = \Sigma\|F_o| - |F_c\|/\Sigma|F_o|$ and $R_w = [\Sigma w(|F_o| - |F_c|)^2/\Sigma w|F_o|^2]^{1/2}$. GOF = Estimated standard deviation of unit weight observation.

following the procedure of King and Finger (1979). Initial unit-cell refinements were made without constraints (i.e., as triclinic) to test for deviations from hexagonal dimensionality. At all pressures a and b were within 2 esd of each other, α and β were within 2 esd of 90°, and γ was within 2 esd of 120°. Final cell parameters were calculated with hexagonal constraints (Ralph and Finger, 1982).

An automated Picker four-circle diffractometer operating with filtered MoKα radiation ($\lambda = 0.7107$ Å) was used for all diffraction-intensity measurements. Full sets of intensity data for dolomite were obtained at 0.0, 1.50, 2.90, 3.70, and 4.69 GPa. Intensity data for ankerite were obtained at 0.0, 1.90, 2.97, and 4.00 GPa. All accessible reflections, including crystallographically equivalent reflections, to sin $\theta/\lambda \leq 0.7$ were obtained by the ω-scan technique with 0.025° steps and counting times of 4.0 s per step. Corrections were made for L_p effects and absorption by the components of the diamond-anvil cell. Absorption corrections for the crystal were made with program Absorb (Burnham, 1966), yielding minimum and maximum transmission factors of 90 and 93% for dolomite and 88 and 91% for ankerite. A reflection was considered unobserved when $I < 2$ σ_I. Absorption-corrected data were symmetry averaged prior to each refinement, resulting in approximately 110 (dolomite) or 90 (ankerite) independent observations at each pressure.

Structure refinements

Refinements were carried out with the least-squares program RFINE6, a development version of RFINE4 (Finger and Prince, 1975), which incorporates an option for refining the fraction of a twin given the parent-twin law. The twin fraction of the ankerite crystal used in this study, determined from intensity data measured in air [to $\sin(\theta)/\lambda = 0.7$ and including three asymmetric units], is 27%. In the refinements with data obtained at high pressure, the twin fraction was therefore set equal to 27%. For dolomite and ankerite, a weight of $1/(\sigma_F^2)$ was assigned to each reflection, where σ_F is based on counting statistics. The refinements were initiated with the atomic coordinates of Reeder and Markgraf (1986) for Eugui dolomite and those of Reeder and Dollase (1989) for ankerite sample AMNH 8059. Atomic scattering curves for neutral atoms and corrections for anomalous dispersion were taken from *International Tables for X-ray Crystallogra-*

TABLE 2. Data measurement and refinement information for ankerite at several pressures

Pressure (GPa)	No. ind. obs. ($>2\sigma_i$)	R	R_w	GOF
0.00	81	0.024	0.014	1.32
1.90	84	0.025	0.017	1.80
2.97	83	0.025	0.018	1.20
4.00	91	0.022	0.014	1.30

Note: $R = \Sigma \|F_o| - |F_c\|/\Sigma|F_o|$ and $R_w = [\Sigma w(|F_o| - |F_c|)^2/\Sigma w|F_o|^2]^{1/2}$. GOF = Estimated standard deviation of unit weight observation.

TABLE 4. Positional coordinates and isotropic temperature factors, B (Å²), of ankerite at several pressures

Pressure (GPa)	0.00	1.90	2.97	4.00
A (Ca)				
B	1.10(6)	1.26(8)	0.96(7)	1.00(5)
B (Mg,Fe)				
B	0.36(5)	0.34(6)	0.83(5)	0.66(4)
C				
z	0.2443(8)	0.2432(9)	0.2444(8)	0.2441(6)
B	0.88(10)	0.95(15)	0.84(9)	0.89(10)
O				
x	0.2511(6)	0.2519(7)	0.2523(5)	0.2520(5)
y	−0.0289(6)	−0.0292(10)	−0.0291(6)	−0.0290(7)
z	0.2450(2)	0.2455(2)	0.2452(2)	0.2453(2)
B	1.10(5)	1.17(7)	1.03(5)	1.04(5)

Note: Numbers in parentheses represent estimated standard deviation in the last decimal place quoted.

phy (1974). Final refinements of dolomite included an isotropic extinction correction, assuming type I behavior and a Lorentzian mosaic angular distribution (Becker and Coppens, 1974). An extinction correction in the final refinements of ankerite was omitted because the estimated standard deviation of the refineable extinction parameter, **g**, was the same magnitude as **g**. Details of the refinements of dolomite and ankerite are recorded in Tables 1 and 2, and the refined positional and thermal parameters are presented in Tables 3 and 4. Observed and calculated structure factors for each high-pressure refinement of dolomite and ankerite are listed in Tables 5 and 6, respectively.[1]

RESULTS

Unit-cell parameters

The unit-cell parameters for dolomite and ankerite at several pressures are presented in Tables 7 and 8, respectively. The room pressure values of Eugui dolomite compare well with those reported by Reeder and Markgraf (1986), $a = 4.8069(9)$ Å and $c = 16.002(1)$ Å, and the ankerite cell parameters show reasonable agreement with those of Reeder and Dollase (1989), $a = 4.8312(2)$ Å and $c = 16.166(3)$ Å. The axial compressibilities, a/a_0 and c/c_0, of dolomite and ankerite are plotted as a function

[1] To obtain a copy of Tables 5 and 6, order Document AM-92-491 from the Business Office, Mineralogical Society of America, 1130 Seventeenth Street NW, Suite 330, Washington, DC 20036, U.S.A. Please remit $5.00 in advance for the microfiche.

of pressure in Figure 1. The mean (linear) compressibilities of the a and c axes of dolomite are 1.922×10^{-3}/GPa and 5.823×10^{-3}/GPa, respectively. Ankerite displays similar values, as 1.903×10^{-3}/GPa is the compressibility of a and 6.083×10^{-3}/GPa is the compressibility of c. Thus for both dolomite and ankerite, c is approximately three times as compressible as a. The axial ratio, c/a, therefore decreases with pressure.

The variation of the molar volume of dolomite and ankerite with pressure is shown in Figure 2. Isothermal bulk moduli of dolomite and ankerite, determined from linear regressions of the pressure-volume data and by setting V/V_0 equal to 1.00 at room pressure, are 102(1) and 98(1) GPa, respectively. Alternatively, the isothermal bulk modulus of each crystal can be determined from a least-squares fit of a Birch-Murnaghan equation of state. By constraining V/V_0 to 1.00 at room pressure and setting K'_0 equal to 4, one obtains values of 94.1(7) and 91.7(4) GPa for the isothermal bulk moduli of dolomite and ankerite, respectively. Thus both methods show that the bulk modulus of the ferroan dolomite is very similar to that of the pure Mg-end-member dolomite, with the ferroan dolomite marginally more compressible than pure dolomite.

TABLE 3. Positional coordinates and isotropic temperature factors, B (Å²), of dolomite at several pressures

Pressure (GPa)	0.00	1.50	2.90	3.70	4.69
A (Ca)					
B	0.71(3)	0.79(6)	0.88(6)	0.84(5)	0.76(6)
B (Mg)					
B	0.50(4)	0.46(8)	0.50(7)	0.42(6)	0.46(8)
C					
z	0.2431(3)	0.2434(6)	0.2426(6)	0.2416(4)	0.2439(8)
B	0.73(7)	0.87(13)	0.68(11)	0.47(9)	0.65(11)
O					
x	0.2482(4)	0.2485(7)	0.2488(6)	0.2496(5)	0.2496(6)
y	−0.0357(4)	−0.0355(7)	−0.0359(6)	−0.0359(5)	−0.0359(6)
z	0.2440(1)	0.2443(2)	0.2442(2)	0.2443(1)	0.2443(2)
B	0.84(4)	0.93(7)	0.93(6)	0.79(5)	0.82(5)

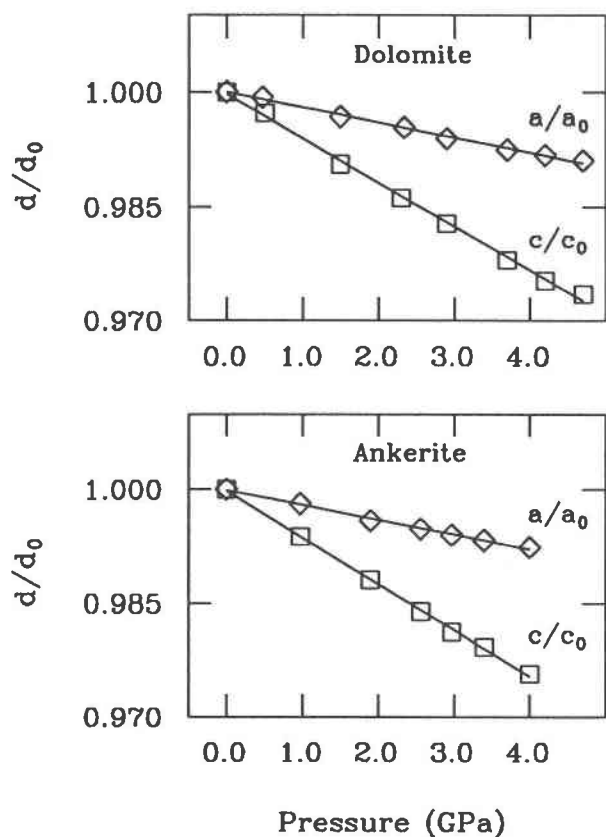*Note:* Numbers in parentheses represent estimated standard deviation in the last decimal place quoted.

Fig. 1.   The variation of a/a_0 and c/c_0 with pressure in dolomite and ankerite.

Fig. 2.   Room-temperature compression of dolomite and ankerite.

Structural changes

The dolomite structure is similar to the calcite structure and consists of layers of metal atoms that alternate with layers of carbonate groups, with the distribution of O atoms approximating a pattern of hexagonal closest packing. The presence of more than one metal atom, A and B, ordered in alternating layers with the carbonate groups in the dolomite structure is consistent with $R\overline{3}$ symmetry rather than the $R\overline{3}c$ symmetry of calcite. Because there is a difference between the larger A-O bond length and the B-O bond length, O lies closer to B rather than A, with the net result that the CO_3 groups within a
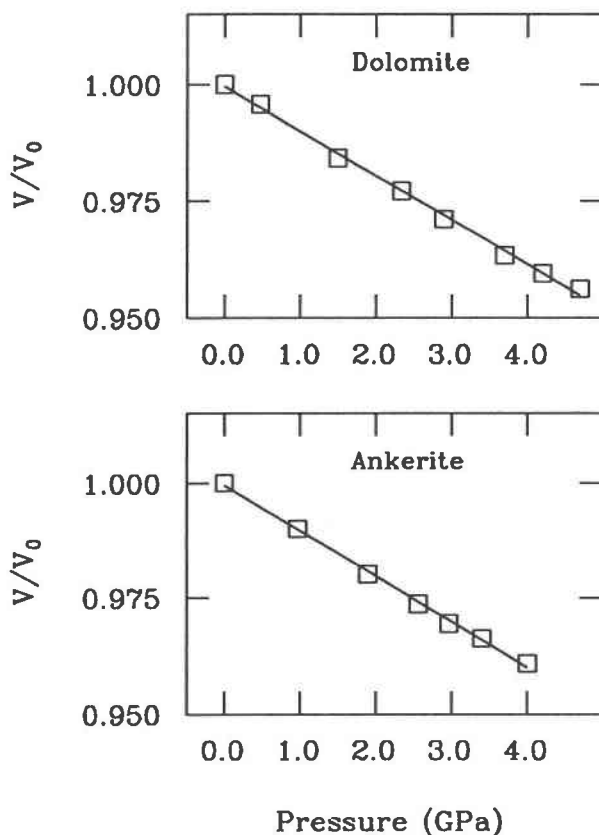
given layer are rotated around their threefold axis relative to their position in calcite. At room pressure, we determined that the angle of rotation in dolomite is approximately 6.5°, in good agreement with Reeder and Markgraf (1986), and the angle of rotation in the ankerite sample is 5.4°, in good agreement with values of Reeder and Dollase (1989). Unlike calcite, the C atom in the $R\overline{3}$ carbonates does not lie in the plane defined by its three neighboring O atoms. This "aplanarity" (distance that the C atom is displaced from the plane formed by three O atoms in the CO_3 group) is between 0.01 and 0.02 Å in dolomite and ankerite at room pressure, in good agree-

TABLE 7.   Unit-cell parameters of dolomite at several pressures

Pressure (GPa)	a (Å)	c (Å)	V (Å³)
0.00	4.8064(5)	16.006(2)	320.22(8)
0.47	4.8028(7)	15.962(2)	318.87(9)
1.50	4.7910(7)	15.856(2)	315.20(9)
2.34	4.7843(9)	15.785(2)	312.90(11)
2.90	4.7777(5)	15.730(1)	310.97(6)
3.70	4.7703(7)	15.653(2)	308.47(10)
4.20	4.7672(6)	15.611(2)	307.24(8)
4.69	4.7636(5)	15.582(3)	306.21(8)

Note: Standard deviations in parentheses.

TABLE 8.   Unit-cell parameters of ankerite at several pressures

Pressure (GPa)	a (Å)	c (Å)	V (Å³)
0.00	4.8360(8)	16.186(2)	327.82(11)
0.97	4.8265(8)	16.085(2)	324.51(11)
1.90	4.8163(6)	15.992(2)	321.26(9)
2.56	4.8109(6)	15.924(2)	319.18(8)
2.97	4.8070(6)	15.881(2)	317.81(8)
3.40	4.8038(8)	15.847(2)	316.71(10)
4.00	4.7990(6)	15.792(2)	314.97(8)

Note: Standard deviations in parentheses.

TABLE 9. Interatomic distances (Å) and angles (°) in dolomite at several pressures

Pressure (GPa)	0.00	1.50	2.90	3.70	4.69
A (Ca)					
A-O	2.381(2)	2.365(3)	2.355(3)	2.345(2)	2.339(3)
O1-O2*	3.297(3)	3.287(5)	3.277(5)	3.267(4)	3.261(4)
O1-O6**	3.436(3)	3.402(6)	3.382(5)	3.365(4)	3.355(6)
O1-A-O2	87.64(5)	88.02(11)	88.19(10)	88.30(8)	88.39(11)
O1-A-O6	92.36(5)	91.98(11)	91.81(10)	91.70(8)	91.61(11)
B (Mg)					
B-O	2.081(2)	2.073(3)	2.060(3)	2.054(2)	2.048(3)
O1-O2*	2.898(3)	2.888(5)	2.875(5)	2.867(4)	2.863(4)
O1-O6**	2.987(3)	2.973(6)	2.951(5)	2.941(4)	2.929(6)
O1-B-O2	88.26(11)	88.34(13)	88.50(11)	88.54(9)	88.69(13)
O1-B-O6	91.74(11)	91.66(13)	91.50(11)	91.46(9)	91.31(13)
A-B	3.8493(5)	3.8256(7)	3.8055(7)	3.7936(7)	3.7826(5)
B-B†	4.8064(5)	4.7910(7)	4.7777(5)	4.7703(7)	4.7636(5)
C					
C-O	1.288(2)	1.284(3)	1.283(3)	1.285(2)	1.283(2)
C-A	3.129(2)	3.112(5)	3.106(4)	3.106(4)	3.083(5)
C-B	3.032(2)	3.022(4)	3.006(4)	2.994(3)	3.002(5)
C-A‡	3.890(5)	3.860(10)	3.816(9)	3.782(7)	3.800(12)
C-B‡	4.113(5)	4.068(10)	4.049(9)	4.044(7)	3.990(12)

Note: Standard deviations in parentheses.
 * Basal edge of octahedron.
 ** Lateral edge of octahedron.
 † The distance *d* (B-B) = *d* (A-A) = *a*.
 ‡ Distance along threefold axis.

ment with values of Reeder and Markgraf (1986) and Reeder and Dollase (1989). The A and B cations are octahedrally coordinated to six O atoms, which in turn are collectively bonded to six different metal atoms and six different C atoms. Thus the structure can be described in terms of polyhedral linkages as consisting of corner-sharing octahedra and trigonal carbonate units. We describe below the effect of pressure on the carbonate groups, cat-

TABLE 10. Interatomic distances (Å) and angles (°) in ankerite at several pressures

Pressure (GPa)	0.00	1.90	2.97	4.00
A (Ca)				
A-O	2.373(3)	2.350(4)	2.343(3)	2.336(3)
O1-O2*	3.280(4)	3.264(6)	3.257(4)	3.251(4)
O1-O6**	3.429(5)	3.383(6)	3.373(5)	3.354(4)
O1-A-O2	87.45(9)	87.96(12)	88.01(10)	88.21(9)
O1-A-O6	92.55(9)	92.04(12)	91.99(10)	91.79(9)
B (Mg,Fe)				
B-O	2.126(3)	2.113(4)	2.102(3)	2.097(3)
O1-O2*	2.956(4)	2.936(7)	2.929(4)	2.927(4)
O1-O6**	3.056(4)	3.039(6)	3.013(5)	3.005(4)
O1-B-O2	88.07(10)	88.04(13)	88.35(11)	88.51(10)
O1-B-O6	91.93(10)	91.96(13)	91.65(11)	91.49(10)
A-B	3.8823(8)	3.8518(6)	3.8351(6)	3.8216(6)
B-B†	4.8360(8)	4.8163(6)	4.8070(6)	4.7990(6)
C				
C-O	1.290(2)	1.290(3)	1.288(2)	1.285(2)
C-A	3.142(6)	3.132(6)	3.114(6)	3.108(5)
C-B	3.062(6)	3.038(6)	3.037(5)	3.029(4)
C-A‡	3.953(14)	3.890(14)	3.881(13)	3.855(10)
C-B‡	4.139(14)	4.106(14)	4.060(13)	4.041(10)

Note: Standard deviations in parentheses.
 * Basal edge of octahedron.
 ** Lateral edge of octahedron.
 † The distance *d* (B-B) = *d* (A-A) = *a*.
 ‡ Distance along threefold axis.

ion octahedra, and nonbonded interactions in the structure.

The carbonate groups in dolomite and ankerite are incompressible, rigid units. As shown in Tables 9 and 10, the C-O distance does not vary by more than 2 esd between room pressure and 4.7 GPa for either dolomite or ankerite. In addition, the *z* coordinates of the C and O atoms do not change significantly with pressure in either dolomite or ankerite (Tables 3 and 4), suggesting that the aplanarity of the carbonate group does not change significantly between room pressure and 4.69 GPa. Our results further suggest that the rotation angle of the CO_3 groups in dolomite does not show a significant change with pressure; in dolomite the rotation angle is 6.6° at each pressure. In ankerite, the rotation angle is 5.4° at all pressures of this study except at 1.90 GPa, where it is slightly higher, 5.7°. We should point out that there may be subtle changes in these parameters with pressure that may not be resolvable in the current experiments given the restricted access to reciprocal space in these high-pressure experiments (e.g., Hazen and Finger, 1982). Increased precision in the positional parameters could be obtained from measurement of more than one data set at the same pressure with the crystal in different, nonsymmetry-equivalent orientations, as described by Angel (1988).

Unlike the carbonate groups, the cation octahedra show significant compression in dolomite and ankerite. In both compounds, the larger AO_6 octahedron is slightly more compressible than the BO_6 octahedron (Figs. 3 and 4). In addition, the compressibilities of the AO_6 octahedra in dolomite and ankerite are almost identical, as are those of the BO_6 octahedra. The (linear) compressibilities of A-O and B-O in dolomite, for example, are 3.77×10^{-3}/GPa and 3.52×10^{-3}/GPa, respectively. In ankerite, the
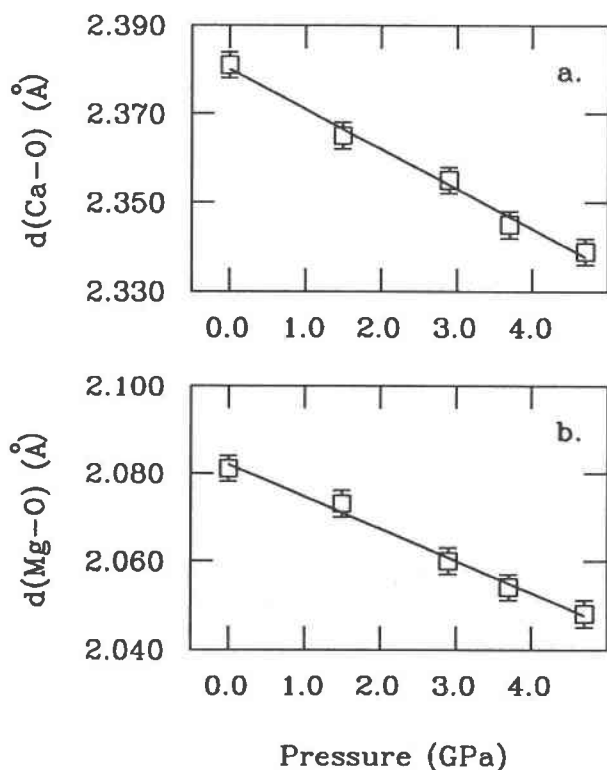
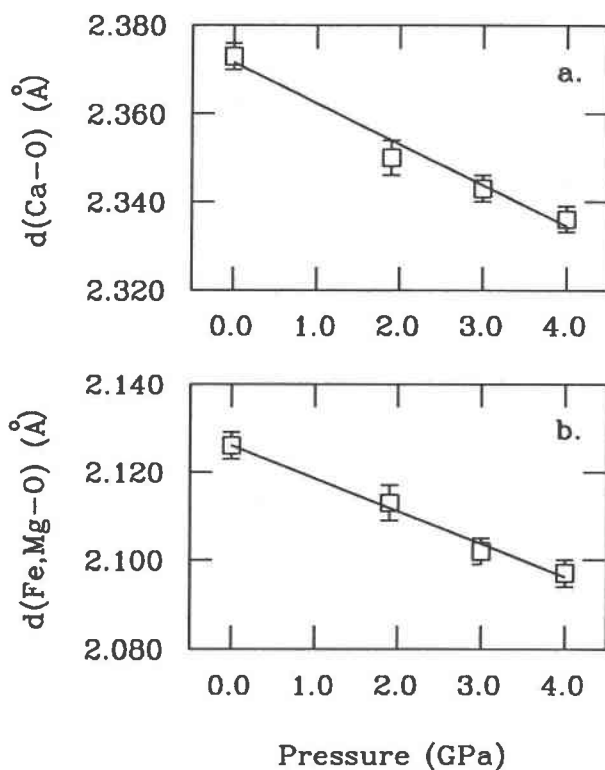Fig. 3. Variation of (a) Ca-O bond lengths and (b) Mg-O bond lengths with pressure in dolomite.

Fig. 4. Variation of (a) Ca-O bond lengths and (b) (Fe,Mg)-O bond lengths with pressure in ankerite.

compressibility of A-O, 3.93×10^{-3}/GPa, is also slightly larger than B-O, 3.51×10^{-3}/GPa. It is not surprising, therefore, that the polyhedral bulk moduli of AO_6 and BO_6 are similar. Polyhedral bulk moduli of AO_6 and BO_6 in dolomite as calculated from a linear regression of the pressure-octahedral volume data are 91 and 98 GPa, respectively (Table 11). The polyhedral bulk moduli of AO_6 and BO_6 in ankerite calculated from the data in Table 12 are 89 and 101 GPa, respectively. Thus compressibilities of the M-O bonds of the two structures are almost identical, as are the bulk moduli of dolomite and ankerite.

At room pressure and temperature, the two cation octahedra in dolomite and ankerite are trigonally distorted by elongation along the threefold axis. In both compounds, the larger A octahedron is slightly more distorted than the smaller B octahedron, as shown by the quadratic

elongation (Robinson et al., 1971) values given in Tables 11 and 12. The values determined in this study at room pressure are in excellent agreement with the values of Reeder and Markgraf (1986) and Reeder and Dollase (1989). It should be noted that the absolute values of the distortions involved are very small and the cation octahedra in dolomite and ankerite are nearly regular. With increasing pressure, there is a suggestion that the distortion of the AO_6 octahedron decreases slightly in dolomite and ankerite, whereas there is no discernible change in the quadratic elongation values of the BO_6 octahedra (Tables 11 and 12). The changes in O-M-O angles within octahedra (Tables 9 and 10) show a trend of decreasing trigonal distortion with increasing pressure more clearly, but again the absolute change is very small. For example, O1-Ca-O2 (O atoms 1 and 2 are in the same layer) in-

TABLE 11. Octahedral volumes (V_P) and quadratic elongation (QE) values of the AO_6 and BO_6 polyhedra in dolomite at several pressures

Pressure (GPa)	0.00	1.50	2.90	3.70	4.69
A (Ca)					
V_P (Å³)	17.95(3)	17.61(3)	17.38(3)	17.16(2)	17.06(3)
QE	1.0017(5)	1.0012(6)	1.0010(5)	1.0009(4)	1.0008(5)
B (Mg)					
V_P (Å³)	12.00(2)	11.85(2)	11.65(2)	11.53(2)	11.45(2)
QE	1.0009(16)	1.0008(16)	1.0007(16)	1.0006(16)	1.0005(16)

Note: Standard deviations in parentheses.

TABLE 12. Octahedral volumes (V_P) and quadratic elongation (QE) values of the AO_6 and BO_6 polyhedra in ankerite at several pressures

Pressure (GPa)	0.00	1.90	2.97	4.00
A (Ca)				
V_P (Å³)	17.76(3)	17.28(4)	17.13(3)	16.96(3)
QE	1.0019(5)	1.0012(7)	1.0012(5)	1.0010(5)
B (Mg,Fe)				
V_P (Å³)	12.78(2)	12.55(3)	12.37(2)	12.29(2)
QE	1.0011(16)	1.0011(16)	1.0008(16)	1.0007(16)

Note: Standard deviations in parentheses.

creases from 87.70(9)° at room pressure to 88.4(1)° at 4.69 GPa in dolomite and from 87.45(9)° at room pressure to 88.21(9)° at 4.00 GPa in ankerite. The O1-(Mg,Fe)-O2 angles also increase with pressure. The angle increases from 88.2(1)° to 88.7(1)° between room pressure and 4.69 GPa in dolomite and from 88.1(1)° to 88.5(1)° between room pressure and 4.00 GPa in ankerite. The net result is that at higher pressures the O-M-O angles of the octahedra are marginally closer to 90° than at lower pressures.

The basis for these trends in polyhedral distortion is reflected in the compressibilities of the O-O interatomic distances within the octahedra. It is apparent from Tables 9 and 10 that, although the lateral edge lengths (O1-O6 distance) of the CaO_6 octahedron of the two carbonates are not significantly different, the basal edge (O1-O2 distance) is significantly shorter in ankerite than dolomite. At high pressure, the basal edge of the CaO_6 octahedron in ankerite is still shorter than in dolomite but by the same amount observed at room pressure. For the AO_6 octahedron in dolomite, the (linear) compressibilities of the lateral edge (O1-O6) and basal edge (O1-O2) of the AO_6 octahedron are 5.10×10^{-3}/GPa and 2.16×10^{-3}/GPa, respectively. Similar trends are observed in the AO_6 octahedron of ankerite. The (linear) compressibilities of the lateral and basal edges are 5.36×10^{-3}/GPa and 2.23×10^{-3}/GPa, respectively. The basal and lateral edge lengths of the BO_6 in ankerite are larger than those of dolomite, at room pressure and higher pressures, but by approximately the same amount (Tables 9 and 10). For the BO_6 octahedron in dolomite, the compressibilities of the lateral edge and basal edge are 4.42×10^{-3}/GPa and 2.92×10^{-3}/GPa, respectively. Similarly, the compressibility of the lateral edge of the BO_6 octahedron in ankerite, 4.34×10^{-3}/GPa, is greater than the compressibility of the basal edge, 2.57×10^{-3}/GPa. Thus the lateral edge lengths of AO_6 and BO_6 in dolomite and ankerite are more compressible than the basal edge lengths, and the values for both compounds are very similar. There is also a greater difference between the compressibilities of lateral and basal edges in the AO_6 than those of the BO_6 octahedra in both dolomite and ankerite. The decrease in the basal edges of the AO_6 and BO_6 octahedra with pressure control, for the most part, the compression of *a* be-

cause the CO_3 groups are essentially incompressible units. The compression between these O layers, however, is much greater and is reflected in the greater compressibility of *c* relative to *a*.

DISCUSSION

The most significant structural variation with increasing pressure in dolomite and ankerite is the compression of the CaO_6 and $(Mg,Fe)O_6$ octahedra. In contrast, the CO_3 group remains essentially invariant with increasing pressure. No significant change was observed in the C-O distances, the rotation of the CO_3 groups, or the aplanarity of the carbonate groups. Compression of this corner-sharing structure is therefore attributable to polyhedral compression with no polyhedral tilting, as shown by the invariance of the CO_3 rotation angle. The CO_3 group plays an important role in the unit-cell compression. Because the C-O distance is essentially unchanged with pressure and because the CO_3 group is oriented parallel to (0001), compression is greater along *c* than *a*. Compression along *c* is the net effect of compression of the CaO_6 and $(Mg,Fe)O_6$ octahedra.

Hazen and Finger (1979) noted that regardless of structure type, a given type of polyhedron has nearly constant bulk modulus (within 15%), even though the individual bonds within a polyhedron may show a wide range of compressibilities. The polyhedral bulk moduli of the CaO_6 octahedra in dolomite and ankerite, 91 and 89 GPa, are approximately 18% lower than the value derived from compression of CaO (Hazen and Finger, 1982), 110 GPa, and that observed in the CaO_6 octahedra of monticellite (Sharp et al., 1987), 110 GPa. They are closer to the values reported for the Ca site in the clinopyroxenes fassaite (Hazen and Finger, 1977), 90 GPa, and diopside (Levien and Prewitt, 1981), 101 GPa, although the coordination of the M2 site in these compounds is eightfold rather than sixfold. Thus the compressibility of the CaO_6 octahedron in dolomite and ankerite is slightly greater than those for other CaO_6 octahedra.

The MgO_6 octahedron in dolomite is more compressible than would be expected from high-pressure studies of other Mg-bearing compounds. For example, the polyhedral bulk modulus of MgO_6 in dolomite, 98 GPa, is approximately 40% lower than the value derived from compression of MgO (Hazen and Finger, 1982), 161 GPa. Values for MgO_6 octahedra in silicates, however, are variable. Sharp et al. (1987), for example, reported a polyhedral bulk modulus for the MgO_6 octahedron in monticellite of 150 GPa, similar to that for MgO, whereas Hazen (1976) reported values of 120 and 100 GPa for the $M1O_6$ and $M2O_6$ octahedra in forsterite, and a more recent study of forsterite at higher pressures (Kudoh and Takéuchi, 1985) gave values of 140 and 130 GPa. The compressibility of MgO_6 in diopside (Levien and Prewitt, 1981) is 105 GPa. Thus, the MgO_6 and CaO_6 polyhedral bulk moduli in dolomite show the greatest difference with those of the NaCl structure.
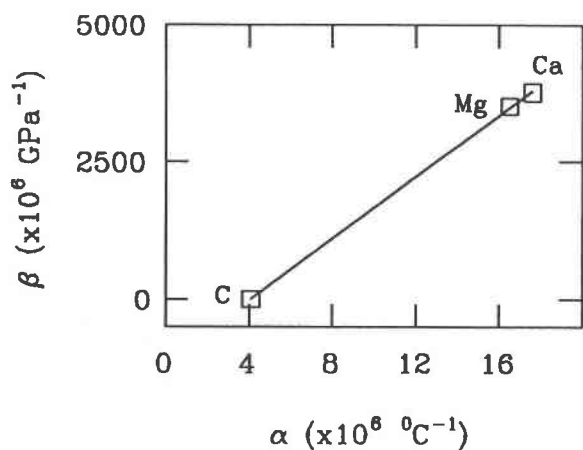
Upon initial inspection, it is not clear why the MgO_6

Fig. 5. Values of α vs. β for the metal-O bonds in dolomite. Note that the values of the C-O, Ca-O, and Mg-O bonds lie along the same line. The slope of the line is 281 °C/GPa.
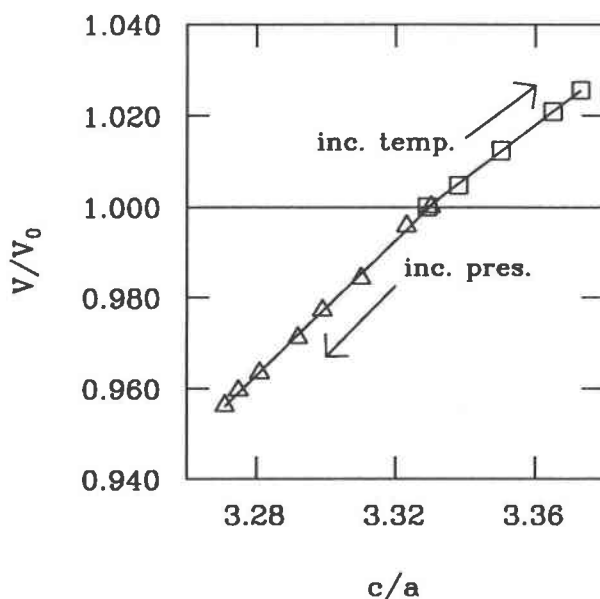

Fig. 6. Variation of c/a with V/V_0 in dolomite at high temperature (squares) and high pressure (triangles). High-temperature data are from Reeder and Markgraf (1986).

and CaO_6 octahedra in dolomite are more compressible than the polyhedra of MgO and CaO, especially since the metal-O bond lengths in dolomite are smaller than those in MgO and CaO. The Ca-O bond length in CaO is 2.406 Å (Hazen and Finger, 1982) compared with 2.381 Å in dolomite, and the Mg-O bond length in MgO is 2.106 Å (Hazen and Finger, 1982) compared with 2.081 Å in dolomite. One explanation for the different octahedral compressibilities may be found in the arrangement of the octahedra in the two structures. Whereas the octahedra in dolomite are exclusively corner sharing, the octahedra in MgO and CaO are exclusively edge sharing. Consequently, the octahedra are more tightly packed in the latter, resulting in smaller metal-metal distances. In MgO, for example, the Mg-Mg distance is 2.978 Å and the Ca-Ca distance in CaO is 3.403 Å, values which are significantly smaller than the Ca-Ca, Ca-Mg, or Mg-Mg distances in dolomite. In dolomite, the shortest Ca-Mg distance is 3.849 Å and the shortest Mg-Mg distance is 4.8064(5) Å (the *a* cell edge), which is also the smallest Ca-Ca distance (Tables 9 and 10). It should be noted that the nearest cation neighbors to an Mg or Ca atom in dolomite and ankerite are the C atoms. The Ca-C distance is 3.128(3) Å and the Mg-C distance is 3.033(3) Å in dolomite. The C atoms, however, are screened from the Mg and Ca atoms by the O atoms bonded to the C atoms. We suggest that metal-metal interactions play a greater role in the compression of NaCl structures than in the dolomite structure, with the result that the polyhedral bulk moduli are larger (i.e., less compressible) in the NaCl structure than in dolomite or ankerite.

Comparison of pressure and temperature effects

Hazen and Prewitt (1977) suggested that in compounds where all component polyhedra have similar values of α/β, the mechanism of compression will be essentially equivalent to that of cooling; in other words, compression

and thermal expansion will have inverse effects. We find, when combining our results with those of Reeder and Markgraf's (1986) high-temperature study, that the component M-O bonds in dolomite lie along a line of constant α/β, as shown in Figure 5. Dolomite should therefore display inverse behavior. Most structural features do, in fact, show opposite trends with pressure and temperature. The c/a ratio, for example, increases with increasing temperature and decreases with increasing pressure, as shown in Figure 6. The *c* axis in dolomite is approximately three times as compressible as *a* and shows approximately four times the expansion of *a* with increasing temperature.

The anisotropy between *c* and *a* is controlled, in large part, by the presence of the carbonate groups that lie in (0001). Neither the rotation angle nor the aplanarity of the CO_3 groups changes significantly with increasing temperature or pressure. However, although no significant change is observed in the C-O bond lengths with pressure, Reeder and Markgraf (1986) found that the libration-corrected C-O bond length increases very slightly but uniformly between 24 and 600 °C and has a mean thermal expansion coefficient (MTEC) of 4.1×10^{-6}/°C.

The structural response of the CaO_6 and MgO_6 octahedra to temperature and pressure controls expansion and compression along *c*. Reeder and Markgraf (1986) determined the MTEC of the Ca-O bond length, 17.6×10^{-6}/°C, and Mg-O bond length, 16.5×10^{-6}/°C. These values, as we found for the bond compressibilities, are very similar, with Ca-O having a slightly greater values than Mg-O. Moreover, the MTEC of MgO_6 is greater than the value of 13.8×10^{-6}/°C that is obtained for Mg in octahedral coordination from Equation 1 in Hazen and Prew-

itt (1977). It is interesting that the MTECs of dolomite and magnesite (Markgraf and Reeder, 1985) are very similar to the value predicted for Mg in eightfold coordination, $16.4 \times 10^{-6}/°C$ (Hazen and Prewitt, 1977). Because of the anomalous expansion and compression behavior of MgO_6 in dolomite, its value of α/β (0.0036 GPa/°C) is much lower than that found for other oxides that cluster (along with Si, Al, and Fe) around 0.0085 GPa/°C (Hazen and Prewitt, 1977). This value, however, is closer to α/β of CaO_6 in dolomite, 0.0047 GPa/°C, which in turn is closer to Hazen and Prewitt's (1977) predicted value, 0.0057 GPa/°C, for Ca in sixfold coordination. Thus the interesting high-temperature and high-pressure behavior of dolomite is due, in large part, to the MgO_6 octahedron, which displays behavior that is generally associated with a "larger" site occupied by such cations such as Ca, Sr, Ba, and Na (see Table 2 in Hazen and Prewitt, 1977).

The distortions of the CaO_6 and MgO_6 octahedra in dolomite, as indicated by the quadratic elongation, show little change with pressure (Tables 11 and 12). Similarly, Reeder and Markgraf (1986) observed no change in the quadratic elongation of the CaO_6 octahedron with temperature. The quadratic elongation of the MgO_6 octahedron, however, shows a small, uniform increase with temperature. Reeder and Markgraf (1986) noted that the basis for these trends in polyhedral distortion is found in the expansions of the O-O distances of the octahedra. They found that the MTEC of the basal edge (O1-O2) in the CaO_6 octahedron, $17.6 \times 10^{-6}/°C$, is essentially identical to the MTEC of the lateral edge (O1-O6), $17.1 \times 10^{-6}/°C$. However, the MTEC of the basal edge in the MgO_6 octahedron, $7.2 \times 10^{-6}/°C$, is substantially different from the MTEC of the lateral edge, $25.3 \times 10^{-6}/°C$. As we noted earlier, the compressibilities of the lateral edges of the CaO_6 and MgO_6 octahedra are greater than those of the basal edges with increasing pressure. Moreover, there is a larger difference between the compressibilities of the lateral and basal edges of the CaO_6 octahedron than the MgO_6 octahedron. Thus although many structural features of dolomite display opposite trends with increasing temperature and pressure, there are some structural changes that do not follow a simple inverse relationship.

Comparison with calcite

Calcite undergoes two displacive-type phase transformations between 0 and 2.2 GPa at room temperature. The high-pressure transition from $CaCO_3$-I to $CaCO_3$-II, which occurs around 1.5 GPa, involves polyhedral tilting and distortion. The rotation of the CO_3 groups leaves the carbonate layers intact, whereas the Ca atoms are alternatively displaced toward and away from a given carbonate layer (Merrill and Bassett, 1975). At approximately 2.2 GPa, $CaCO_3$-II transforms to $CaCO_3$-III (Bridgman, 1939; Merrill and Bassett, 1975). This transition is displacive and involves a significant change in volume (Bridgman, 1939). The structure of $CaCO_3$-III is not known, although Davis (1964) has suggested that the

X-ray diffraction pattern of $CaCO_3$-III may be similar to that of KNO_3-IV. We observed no phase change in either dolomite or ankerite between 0 and 4.7 GPa. Below, we consider some of the differences between the structures that may be responsible for the two vastly different structural responses to pressure.

The most obvious difference between the structures of calcite and dolomite is the presence of two cations in the latter, occupying different sites. The dolomite structure adjusts to the presence of these different cations by rotation of carbonate groups so that the O atoms are closer to the smaller octahedral site. As stated above, the rotation angle of the carbonate groups, relative to those in calcite, is 6.6° in dolomite and 5.4° in ankerite. Moreover, no significant change was observed in the rotation angle of these groups with increasing pressure, whereas the rotation angle changes from 0° in calcite to 11° in $CaCO_3$-II.

A second difference between the structures is the somewhat higher degree of distortion found in the CaO_6 octahedra of calcite as compared with the nearly regular octahedra of dolomite and ankerite. The CaO_6 octahedron in calcite is distorted by elongation parallel to **c** and has a quadratic elongation of 1.0020 (Effenberger et al., 1981; Finger, 1975; Borodin et al., 1979), slightly larger than the quadratic elongation of the cation octahedra of dolomite and ankerite (Tables 11 and 12). This increased distortion is due, in part, to the Ca atom, which has a fairly large ionic radius of 1.00 Å (Shannon and Prewitt, 1969), residing in an octahedral site. Moreover, Reeder (1983) noted that the equivalent isotropic temperature factors (B_{eq}) of calcite are considerably larger than found in other carbonates for all atoms, being especially pronounced for the O atom. Whether the higher degree of distortion and anomalously high temperature factors are related to the complex behavior of calcite at pressure is not known. We suggest that the presence of an additional cation such as Mg in the dolomite structure may stabilize the structure under pressure and prevent greater distortions from occurring in the CaO_6 octahedra. In both dolomite and ankerite, there was a very slight decrease in distortion of the octahedra with increasing pressure. At all pressures studied, the CaO_6 octahedron was always slightly more distorted than the $(Mg,Fe)O_6$ octahedra but by the same amount. In addition, the similar compressibilities of the two cation octahedra in dolomite and ankerite maintain this stabilizing influence of the smaller octahedron over a large pressure range.

CONCLUSIONS

In conclusion, we have found that the structures of dolomite and ankerite do not transform below 5.0 GPa. The compression of the structure is extremely anisotropic, with *c* approximately three times as compressible as *a*. The carbonate groups remain essentially invariant with increasing pressure, and the principal structural change with pressure is compression of the cation octahedra. The CaO_6 octahedra are slightly more compressible than the

$(Mg,Fe)O_6$, with the $(Mg,Fe)O_6$ having a greater compressibility than generally found in other ferromagnesian minerals. The axial compressibilities, bond compressibilities, and bulk moduli of dolomite and ankerite are almost identical. Thus although the substitution of Fe for Mg in the dolomite structure causes structural changes in bond lengths and angles in the structure, the effect of Fe on the compressibility of the structure is minimal.

REFERENCES CITED

Angel, R.J. (1988) High-pressure structure of anorthite. American Mineralogist, 73, 1114–1119.

Barber, D.J., Heard, H.C., and Wenk, H.R. (1981) Deformation of dolomite single crystals from 20°–800°C. Physics and Chemistry of Minerals, 7, 271–286.

Becker, P.J., and Coppens, P. (1974) Extinction within the limit of validity of the Darwin transfer equations. I. General formalisms for primary and secondary extinction and their application to spherical crystals. Acta Crystallographica, A30, 129–147.

Borodin, V.L., Lyntin, V.I., Ilyukhin, V.V., and Belov, N.V. (1979) Isomorphous calcite-otavite series. Soviet Physics Doklady, 24, 226–227.

Bridgman, P.W. (1939) The high-pressure behavior of miscellaneous minerals. American Journal of Science, 37, 7–18.

Burnham, C.W. (1966) Computation of absorption corrections and the significance of end effects. American Mineralogist, 51, 159–167.

Davis, B.L. (1964) X-ray diffraction data on two high-pressure phases of calcium carbonate. Science, 145, 489–491.

Dove, M.T., and Powell, B.M. (1989) Neutron diffraction study of the tricritical orientational order/disorder phase transition in calcite at 1260 K. Physics and Chemistry of Minerals, 16, 503–507.

Effenberger, H., Mereiter, K., and Zemann, J. (1981) Crystal structure refinements of magnesite, calcite, rhodochrosite, siderite, smithsonite, and dolomite, with discussion of some aspects of the stereochemistry of calcite-type carbonates. Zeitschrift für Kristallographie, 156, 233–243.

Finger, L.W. (1975) Least-squares refinement of the rigid-body motion parameters of CO_3 in calcite and magnesite and correlation with lattice vibrations. Carnegie Institution of Washington Year Book, 74, 572–575.

Finger, L.W., and Prince, E. (1975) A system of Fortran IV computer programs for crystal structure computations. U.S. National Bureau of Standards Technical Note 854, 129 p.

Hazen, R.M. (1976) Effects of temperature and pressure on the crystal structure of forsterite. American Mineralogist, 61, 1280–1293.

Hazen, R.M., and Finger, L.W. (1977) Compressibility and crystal structure of Angra dos Reis fassaite to 52 kbar. Carnegie Institution of Washington Year Book, 76, 512–515.

——— (1979) Bulk modulus–volume relationship for cation-anion polyhedra. Journal of Geophysical Research, 84, 6723–6728.

——— (1982) Comparative crystal chemistry. Wiley, New York.

Hazen, R.M., and Prewitt, C.T. (1977) Effects of temperature and pressure on interatomic distances in oxygen-based minerals. American Mineralogist, 62, 309–315.

Ibers, J.A., and Hamilton, W.C., Eds. (1974) International tables for X-ray crystallography, vol. 4. Kynoch Press, Birmingham, England.

Irving, A.J., and Wyllie, P.J. (1973) Melting relations in $CaO-CO_2$ and $MgO-CO_2$ to 36 kilobars with comments on CO_2 in the mantle. Earth and Planetary Science Letters, 20, 220–225.

——— (1975) Subsolidus and melting relations for calcite, magnesite, and the join $CaCO_3-MgCO_3$ to 36 kb. Geochimica et Cosmochimica Acta, 39, 35–53.

King, H.E., and Finger, L.W. (1979) Diffracted beam crystal centering and its application to high-pressure crystallography. Journal of Applied Crystallography, 12, 374–378.

Kudoh, Y., and Takéuchi, Y. (1985) The crystal structure of forsterite Mg_2SiO_4 under high pressure up to 149 kb. Zeitschrift für Kristallographie, 171, 291–302.

Levien, L., and Prewitt, C.T. (1981) High-pressure structural study of diopside. American Mineralogist, 66, 315–323.

Markgraf, S.A., and Reeder, R.J. (1985) High-temperature structure refinements of calcite and magnesite. American Mineralogist, 70, 590–600.

Merrill, L., and Bassett, W.A. (1975) The crystal structure of $CaCO_3$ (II), a high-pressure metastable phase of calcium carbonate. Acta Crystallographica, B31, 343–349.

Ralph, R.L., and Finger, L.W. (1982) A computer program for refinement of crystal orientation matrix and lattice constants from diffractometer data with lattice symmetry constraints. Journal of Applied Crystallography, 15, 537–539.

Redfern, S.A.T., Salje, E., and Navrotsky, A. (1989) High-temperature enthalpy at the orientational order-disorder transition in calcite: Implications for the calcite/aragonite phase equilibrium. Contributions to Mineralogy and Petrology, 101, 479–484.

Reeder, R.J. (1983) Crystal chemistry of the rhombohedral carbonates. In Mineralogical Society of America Reviews in Mineralogy, 11, 1–47.

Reeder, R.J., and Dollase, W.A. (1989) Structural variation in the dolomite-ankerite solid-solution series: An X-ray, Mössbauer, and TEM study. American Mineralogist, 74, 1159–1167.

Reeder, R.J., and Markgraf, S.A. (1986) High-temperature crystal chemistry of dolomite. American Mineralogist, 71, 795–804.

Reeder, R.J., and Wenk, H.R. (1983) Structure refinements of some thermally disordered dolomites. American Mineralogist, 68, 769–776.

Robinson, K., Gibbs, G.V., and Ribbe, P.H. (1971) Quadratic elongation: A quantitative measure of distortion in coordination polyhedra. Science, 172, 567–570.

Shannon, R.D., and Prewitt, C.T. (1969) Effective ionic radii in oxides and fluorides. Acta Crystallographica, B25, 925–945.

Sharp, Z.D., Hazen, R.M., and Finger, L.W. (1987) High-pressure crystal chemistry of monticellite, $CaMgSiO_4$. American Mineralogist, 72, 748–755.